Quantum imaging with N-photon states in position space

E. Brainis
Service OPERA, Université libre de Bruxelles, Avenue F. D. Roosevelt 50, B-1050 Bruxelles, Belgium
ebrainis@ulb.ac.be

Abstract: We investigate the physics of quantum imaging with $N > 2$ entangled photons in position space. It is shown that, in paraxial approximation, the space-time propagation of the quantum state can be described by a generalized Huygens-Fresnel principle for the N-photon wave function. The formalism allows the initial conditions to be set on multiple reference planes, which is very convenient to describe the generation of multiple photon pairs in separate thin crystals. Applications involving state shaping and spatial entanglement swapping are developed.

OCIS codes: (270.0270) Quantum Optics; (070.2580) Paraxial wave optics.

References and links

1. C. Lu, X. Zhou, O. Guhne, W. Gao, J. Zhang, Z. Yuan, A. Goebel, T. Yang, and J. Pan, "Experimental entanglement of six photons in graph states," Nat. Phys. **3**, 91–95 (2007).
2. H. Hübel, D. R. Hamel, A. Fedrizzi, S. Ramelow, K. J. Resch, and T. Jennewein, "Direct generation of photon triplets using cascaded photon-pair sources," Nature **466**, 601–603 (2010).
3. E. Waks, E. Diamanti, and Y. Yamamoto, "Generation of photon number states," New J. Phys. **8**, 4–8 (2006).
4. W.-B. Gao, C.-Y. Lu, X.-C. Yao, P. Xu, O. Gühne, A. Goebel, Y.-A. Chen, C.-Z. Peng, Z.-B. Chen, and J.-W. Pan, "Experimental demonstration of a hyper-entangled ten-qubit Schrödinger cat state," Nat. Phys. **6**, 331–335 (2010).
5. T. Nagata, R. Okamoto, J. L. O'Brien, K. Sasaki, and S. Takeuchi, "Beating the Standard Quantum Limit with Four-Entangled Photons," Science **316**, 726–729 (2007).
6. R. Okamoto, H. F. Hofmann, T. Nagata, J. L. O'Brien, K. Sasaki, and S. Takeuchi, "Beating the standard quantum limit: phase super-sensitivity of N-photon interferometers," New J. Phys. **10**, 073033 (2008).
7. J.-W. Pan, Z.-B. Chen, C.-Y. Lu, H. Weinfurter, A. Zeilinger, and M. Zukowski, "Multi-photon entanglement and interferometry," to appear in Rev. Mod. Phys. (2011).
8. S. P. Walborn, C. H. Monken, S. Pádua, and P. H. Souto Ribeiro, "Spatial correlations in parametric down-conversion," Phys. Rep. **495**, 87–139 (2010).
9. L. Neves, S. Pádua, and C. Saavedra, "Controlled generation of maximally entangled qudits using twin photons," Phys. Rev. A **69**, 042305 (2004).
10. L. Neves, G. Lima, J. G. Aguirre Gómez, C. H. Monken, C. Saavedra, and S. Pádua, "Generation of entangled states of qudits using twin photons," Phys. Rev. Lett. **94**, 100501 (2005).
11. R. Shimizu, K. Edamatsu, and T. Itoh, "Quantum diffraction and interference of spatially correlated photon pairs and its Fourier-optical analysis," Phys. Rev. A **74**, 013801 (2006).
12. W. H. Peeters, J. J. Renema, and M. P. van Exter, "Engineering of two-photon spatial quantum correlations behind a double slit," Phys. Rev. A **79**, 043817 (2009).
13. G. Lima, A. Vargas, L. Neves, R. Guzmán, and C. Saavedra, "Manipulating spatial qudit states with programmable optical devices," Opt. Express **17**, 10688–10696 (2009).
14. C. Bonato, S. Bonora, A. Chiuri, P. Mataloni, G. Milani, G. Vallone, and P. Villoresi, "Phase control of a path-entangled photon state by a deformable membrane mirror," J. Opt. Soc. Am. B **27**, A175–A180 (2010).
15. A. N. Boto, P. Kok, D. S. Abrams, S. L. Braunstein, C. P. Williams, and J. P. Dowling, "Quantum interferometric optical lithography: Exploiting entanglement to beat the diffraction limit," Phys. Rev. Lett. **85**, 2733–2736 (2000).
16. P. Kok, A. N. Boto, D. S. Abrams, C. P. Williams, S. L. Braunstein, and J. P. Dowling, "Quantum-interferometric optical lithography: Towards arbitrary two-dimensional patterns," Phys. Rev. A **63**, 063407 (2001).

17. D. V. Strekalov, A. V. Sergienko, D. N. Klyshko, and Y. H. Shih, "Observation of two-photon "ghost" interference and diffraction," Phys. Rev. Lett. **74**, 3600–3603 (1995).
18. T. B. Pittman, Y. H. Shih, D. V. Strekalov, and A. V. Sergienko, "Optical imaging by means of two-photon quantum entanglement," Phys. Rev. A **52**, R3429–R3432 (1995).
19. T. B. Pittman, D. V. Strekalov, D. N. Klyshko, M. H. Rubin, A. V. Sergienko, and Y. H. Shih, "Two-photon geometric optics," Phys. Rev. A **53**, 2804–2815 (1996).
20. T. E. Keller, M. H. Rubin, Y. Shih, and L.-A. Wu, "Theory of the three-photon entangled state," Phys. Rev. A **57**, 2076–2079 (1998).
21. J. Wen, E. Oh, and S. Du, "Tripartite entanglement generation via four-wave mixings: narrowband triphoton W state," J. Opt. Soc. Am. B **27**, A11–A20 (2010).
22. J. Wen, M. H. Rubin, and Y. Shih, "Transverse correlations in multiphoton entanglement," Phys. Rev. A **76**, 045802 (2007).
23. J. Wen, P. Xu, M. H. Rubin, and Y. Shih, "Transverse correlations in triphoton entanglement: Geometrical and physical optics," Phys. Rev. A **76**, 023828 (2007).
24. J. Wen and M. H. Rubin, "Distinction of tripartite Greenberger-Horne-Zeilinger and *W* states entangled in time (or energy) and space," Phys. Rev. A **79**, 025802 (2009).
25. J. Wen, S. Du, and M. Xiao, "Improving spatial resolution in quantum imaging beyond the Rayleigh diffraction limit using multiphoton W entangled states," Phys. Lett. A **374**, 3908 – 3911 (2010).
26. B. E. A. Saleh, A. F. Abouraddy, A. V. Sergienko, and M. C. Teich, "Duality between partial coherence and partial entanglement," Phys. Rev. A **62**, 043816 (2000).
27. A. F. Abouraddy, B. E. A. Saleh, A. V. Sergienko, and M. C. Teich, "Role of entanglement in two-photon imaging," Phys. Rev. Lett. **87**, 123602 (2001).
28. A. F. Abouraddy, B. E. A. Saleh, A. V. Sergienko, and M. C. Teich, "Entangled-photon Fourier optics," J. Opt. Soc. Am. B **19**, 1174–1184 (2002).
29. M. Hawton, "Photon position operator with commuting components," Phys. Rev. A **59**, 954–959 (1999).
30. M. Hawton and W. E. Baylis, "Photon position operators and localized bases," Phys. Rev. A **64**, 012101 (2001).
31. M. Hawton, "Photon wave functions in a localized coordinate space basis," Phys. Rev. A **59**, 3223–3227 (1999).
32. I. Bialynicki-Birula, "On the wave function of the photon," Acta Phys. Pol. A **86**, 97–116 (1994).
33. I. Bialynicki-Birula, "Photon wave function," in *Progress in Optics*, vol. 36, E. Wolf, ed. (North-Holland, Elsevier, Amsterdam, 1996), chap. 5, pp. 248–294.
34. J. E. Sipe, "Photon wave functions," Phys. Rev. A **52**, 1875–1883 (1995).
35. Note that the quantum mechanical scalar product $\langle \Psi^{(2)} | \Psi^{(1)} \rangle = \sum_{h=\pm} \int \mathrm{d}^3k [f_{\pm}^{(2)}(\mathbf{k})]^* f_{\pm}^{(1)}(\mathbf{k}) = \int \mathrm{d}^3 r_1 \int \mathrm{d}^3 r_2 [\mathbf{\Psi}^{(2)}(\mathbf{r}_2)]^* \cdot \mathbf{\Psi}^{(1)}(\mathbf{r}_1) \mathscr{W}(\mathbf{r}_1 - \mathbf{r}_2)$ is evaluate using a double integral in the position representation with a non local kernel $\mathscr{W}(\boldsymbol{\rho}) = (\hbar c 2\pi^2 |\boldsymbol{\rho}|^2)^{-1}$.
36. B. J. Smith and M. G. Raymer, "Two-photon wave mechanics," Phys. Rev. A **74**, 062104 (2006).
37. B. J. Smith and M. G. Raymer, "Photon wave functions, wave-packet quantization of light, and coherence theory," New J. Phys. **9**, 414 (2007).
38. J. W. Goodman, *Introduction to Fourier Optics* (Roberts & Company, Englewood, 2005), 3rd ed.
39. In [26, 28], time is only introduced to account for the bandwidth of the continuous biphoton stream and compute coincidence rates in the slow detector limit.
40. T. Legero, T. Wilk, M. Hennrich, G. Rempe, and A. Kuhn, "Quantum beat of two single photons," Phys. Rev. Lett. **93**, 070503 (2004).
41. J. D. Franson, "Bell inequality for position and time," Phys. Rev. Lett. **62**, 2205–2208 (1989).
42. V. Giovannetti, S. Lloyd, L. Maccone, and J. H. Shapiro, "Sub-Rayleigh-diffraction-bound quantum imaging," Phys. Rev. A **79**, 013827 (2009).
43. E. Brainis, C. Muldoon, L. Brandt, and A. Kuhn, "Coherent imaging of extended objects," Opt. Commun. **282**, 465–472 (2009).
44. G. Taguchi, T. Dougakiuchi, N. Yoshimoto, K. Kasai, M. Iinuma, H. F. Hofmann, and Y. Kadoya, "Measurement and control of spatial qubits generated by passing photons through double slits," Phys. Rev. A **78**, 012307 (2008).
45. M. A. Solis-Prosser and L. Neves, "Remote state preparation of spatial qubits," Phys. Rev. A **84**, 012330 (2011).
46. S. P. Walborn, D. S. Ether, R. L. de Matos Filho, and N. Zagury, "Quantum teleportation of the angular spectrum of a single-photon field," Phys. Rev. A **76**, 033801 (2007).
47. P. L. Saldanha and C. H. Monken, "Interaction between light and matter: a photon wave function approach," New J. Phys. **13**, 073015 (2011).
48. J.-W. Pan, D. Bouwmeester, H. Weinfurter, and A. Zeilinger, "Experimental entanglement swapping: Entangling photons that never interacted," Phys. Rev. Lett. **80**, 3891–3894 (1998).
49. N. J. Cerf, M. Lévy, and G. V. Assche, "Quantum distribution of gaussian keys using squeezed states," Phys. Rev. A **63**, 052311 (2001).
50. M. P. Almeida, S. P. Walborn, and P. H. Souto Ribeiro, "Experimental investigation of quantum key distribution with position and momentum of photon pairs," Phys. Rev. A **72**, 022313 (2005).
51. L. Zhang, C. Silberhorn, and I. A. Walmsley, "Secure quantum key distribution using continuous variables of single photons," Phys. Rev. Lett. **100**, 110504 (2008).

52. D. S. Tasca, R. M. Gomes, F. Toscano, P. H. Souto Ribeiro, and S. P. Walborn, "Continuous-variable quantum computation with spatial degrees of freedom of photons," Phys. Rev. A **83**, 052325 (2011).
53. G. Molina-Terriza, J. P. Torres, and L. Torner, "Twisted photons," Nat. Phys. **3**, 305–310 (2007).
54. B.-J. Pors, F. Miatto, G. W. 't Hooft, E. R. Eliel, and J. P. Woerdman, "High-dimensional entanglement with orbital-angular-momentum states of light," J. Opt. **13**, 064008 (2011).

1. Introduction

In the recent years, there has been a growing interest in producing quantum states of light in which more than two photons are entangled. So far, up to six time-entangled photons have been produced through entanglement swapping [1] and photon triplets start being produced through cascaded nonlinear processes [2] or photon number post-selection in a single parametric process [3]. Multi-photon interferometry techniques have been developed to demonstrate the hyper-entanglement of a large number of qubits [4] as well as phase super-sensitivity [5, 6] (for a recent revue on N-photon entanglement and interferometry see [7]). *Spatial* entanglement [8] is particularly interesting for quantum information processing and communication because large Hilbert spaces can be easily manipulated using passive masks or active spatial light modulator [9–14]. It can also be used to improve imaging resolution (quantum super-resolution imaging, quantum lithography) [15, 16] and produce distributed or "ghost" images [17–19]. Schemes to realise spatial N-photon entanglement (with $N > 2$) have been proposed [20, 21]. One can foresee that the manipulation of spatial entanglement of few-photon states of light [22–25] will become an important research field in the forthcoming decade.

In this work, we investigate the physics of quantum imaging with $N > 2$ entangled photons. We describe the quantum state of the electromagnetic field using a N-particle wave function in *position* representation. Position representation is preferred to momentum representation because photon-position is what is actually detected by the photon-counters in a quantum optics experiment. However, in many experiments on spatial entanglement that have been performed so far, photons are generated by spontaneous parametric down-conversion in a nonlinear crystal and detected in the crystal far-field; in this particular case, people usually prefer working in momentum representation of the photon state since the position correlations in the far-field mimic the momentum correlations in the nonlinear crystal plane. In the case of an arbitrary optical system (made of lenses, mirror, masks, beam splitters, ...) between the crystal plane and the detection region, the use of the momentum representation for the field in the crystal plane will involve mixed propagators $g(\mathbf{k}, \mathbf{r}_j)$, where $\mathbf{r}_j$ are the positions of the photon-counters and $\mathbf{k}$ wave vectors [22, 23]. Such propagators arise because the photons generated through nonlinear interactions are first regarded as populating an ensemble of plane-wave modes (momentum representation). Then, when it comes to calculate the joint detection probabilities at some selected positions, the local interference of all these modes (that is the position representation) is calculated. Instead, if position representation is chosen from the beginning, the propagators have the usual and intuitive point-to-point form $h(\mathbf{r}, \mathbf{r}_j)$. For applications of the photon position representation to quantum imaging problems with bi-photons ($N = 2$), see [11, 12].

Application of standard Fourier optics techniques to the position representation wave function shows that the propagation of N photons through an optical system can be described by a generalized Huygens-Fresnel principle. This has been first noticed for biphoton states produced by parametric down-conversion in nonlinear crystals [26–28]. Our generalization to N-photon states brings new interesting features: (i) it introduces time in the diffraction integral (giving a space-time picture of entanglement propagation), (ii) it shows how to deal with interferometers in the photon path, and most importantly (iii) the formalism applies to quantum systems made of an arbitrary number of photons, possibly emitted by sources that are located in *different* transverse planes Σ_j. To our best knowledge, this last situation has never been considered

before in the context of quantum imaging despite its practical importance (see the generation scheme in [1], for instance).

The article is organized as follows. In Sec. 2, we review the foundations of the position wave function representation of light. Then, we turn to paraxial approximation, derive the generalized Huygens-Fresnel principle (Sec. 3) and discuss the connection between the photon wave function and photodetection probabilities (Sec. 4). Finally, in Sec. 5 and 6, we apply the general formalism to specific examples. The example of Sec. 5 shows how an initial 3-photon position entanglement can be used to shape a 2-photon wave function through the detection of the third photon. In Sec. 6, we analyse an entanglement-swapping scheme acting on a pair of bi-photons produced in two different nonlinear crystals: combining the detection of two photons with wave front shaping of remaining two photons, entangled images can be created.

2. Photon wave functions in position representation

The *position* wave function of a photon is defined as the projection of the state vector on localized particle states (the eigenstates of the photon position operator $\hat{\mathbf{r}}$) [29]. The very existence of such an operator for photons and the problem of photon localization has been a long standing debate that received a satisfying solution only recently. The existence of a proper photon position operator $\hat{\mathbf{r}}$ that has commuting Hermitian Cartesian components satisfying $[\hat{r}_k, \hat{p}_l] = i\hbar\delta_{kl}$ ($\hat{\mathbf{p}}$ being the photon momentum) has been proven [29, 30]. The eigenfunctions of $\hat{\mathbf{r}}$ are transverse waves that can be interpreted as localized-photon states [31]. Any admissible single-photon wave function is obtained as a linear combination of these localized states. N-photon wave functions are symmetric elements of the tensor product of N single-particle Hilbert spaces. However, the definition of the position operator $\hat{\mathbf{r}}$ is *not* unique. Therefore, there is more than one way to assign a position wave function to a single photon. The most popular one is probably the so-called Bialynicki-Birula-Sipe wave function $\overline{\psi}(\mathbf{r},t) = [\boldsymbol{\psi}_+(\mathbf{r},t)\ \boldsymbol{\psi}_-(\mathbf{r},t)]$ which has two vector components corresponding to photons with positive and negative helicity [32, 33]. Each vector component has a Fourier expansion that reads

$$\boldsymbol{\psi}_\pm(\mathbf{r},t) = \int \mathrm{d}^3k\ \sqrt{\hbar kc}\ \mathbf{e}_\pm(\mathbf{k})\ f_\pm(\mathbf{k})\ \frac{\mathrm{e}^{\mathrm{i}(\mathbf{k}\cdot\mathbf{r}-kc\,t)}}{(2\pi)^{3/2}}, \tag{1}$$

where $k = |\mathbf{k}|$ and $\mathbf{e}_\pm(\mathbf{k})$ are the unit circular polarization vectors for photons propagating in the $\mathbf{k}$-direction. Normalization is such that the complex coefficients $f_\pm$ satisfy $\sum_{h=\pm}\int \mathrm{d}^3k\,|f_h(\mathbf{k})|^2 = 1$. This wave function transforms as an elementary object under Lorentz transformation and can be easily connected to Maxwell fields. In this work, we write the wave function is a slightly different (but equivalent) way that consists in summing both helicity components together:

$$\boldsymbol{\Psi}(\mathbf{r},t) = \boldsymbol{\psi}_+(\mathbf{r},t) + \boldsymbol{\psi}_-(\mathbf{r},t). \tag{2}$$

This provides a vector representation instead of the bi-vector one [34]. Since $\boldsymbol{\psi}_+$ and $\boldsymbol{\psi}_-$ are orthogonally polarized, they never mix: if $\boldsymbol{\Psi}$ is given, $\boldsymbol{\psi}_+$ and $\boldsymbol{\psi}_-$ can be deduced. Therefore the information content in the vector function $\boldsymbol{\Psi}$ is the same as in the bi-vector field $\overline{\psi}$.

Replacing the complex coefficients $f_\pm(\mathbf{k})$ by annihilation operators $\hat{a}_\pm(\mathbf{k})$ in Eq. (1), the fundamental photon field is found to be proportional to the *positive frequency* part of the electric field:

$$\hat{\boldsymbol{\Psi}}(\mathbf{r},t) = \sum_{h=\pm}\int \mathrm{d}^3k\ \sqrt{\hbar kc}\ \mathbf{e}_h(\mathbf{k})\ \hat{a}_h(\mathbf{k})\ \frac{\mathrm{e}^{\mathrm{i}(\mathbf{k}\cdot\mathbf{r}-kc\,t)}}{(2\pi)^{3/2}} = -\mathrm{i}\ \sqrt{2\varepsilon_0}\ \hat{\mathbf{E}}^{(+)}(\mathbf{r},t).$$

Note that $\hat{\boldsymbol{\Psi}} \propto \hat{\mathbf{E}}^{(+)}$ holds information about *both* electric and magnetic field. Therefore, it provides a complete information about electromagnetic configuration. To show this explicitly, one decomposes $\hat{\boldsymbol{\Psi}}$ again into its helicity components $\hat{\boldsymbol{\psi}}_+$ and $\hat{\boldsymbol{\psi}}_-$ and subtract

them: this yields $\hat{\mathbf{B}}^{(+)} = \sqrt{\mu_0/2}(\hat{\boldsymbol{\psi}}_+ - \hat{\boldsymbol{\psi}}_-)$, the positive frequency part of the magnetic field. In the second quantization formalism, the state of a single-photon wave packet writes: $|\Psi\rangle = \sum_{h=\pm} \int \mathrm{d}^3k \; f_h(\mathbf{k}) \; |1_{\mathbf{k},h}\rangle$, where $|1_{\mathbf{k},h}\rangle = a_h^\dagger(\mathbf{k})|0\rangle$ and $f_\pm(\mathbf{k})$ are the same spectral amplitudes that appear in Eq. (1). The connection between the first and second quantization formalism is given by the relation $\boldsymbol{\Psi}(\mathbf{r},t) = \langle 0|\hat{\boldsymbol{\Psi}}(\mathbf{r},t)|\Psi\rangle = -\mathrm{i}\sqrt{2\varepsilon_0}\,\langle 0|\hat{\mathbf{E}}^{(+)}(\mathbf{r},t)|\Psi\rangle$. Since $\langle\Phi|\hat{\boldsymbol{\Psi}}(\mathbf{r},t)|\Psi\rangle = 0$ for all $|\Phi\rangle \neq |0\rangle$, we have $\Psi^*_{i'}(q')\Psi_i(q) = \langle\Psi|\hat{\Psi}^\dagger_{i'}(q')\hat{\Psi}_i(q)|\Psi\rangle = 2\varepsilon_0\langle\hat{E}^{(-)}_{i'}(q')\hat{E}^{(+)}_i(q)\rangle$ for any pair of points $q = (\mathbf{r},t)$ and $q' = (\mathbf{r}',t')$, where the indexes $(i,i') \in \{x,y,z\}^2$ represent Cartesian components. This relates the Bialynicki-Birula-Sipe wave-function to the usual first-order correlation functions of coherence theory. Therefore, in the context of first-order perturbation theory and dipole moment interaction with matter, $|\boldsymbol{\Psi}(\mathbf{r},t)|^2$ is proportional to the photon absorption (detection) probability at point $\mathbf{r}$ at time t (see Sec. 4). In addition, $\int |\boldsymbol{\Psi}(\mathbf{r},t)|^2\mathrm{d}^3r = \langle\Psi|\hat{H}|\Psi\rangle$ is the expectation value of the photon energy [32–34]. As a consequence, $|\boldsymbol{\Psi}(\mathbf{r},t)|^2$ can also be interpreted as a spatial density of electromagnetic energy at time t. Strictly speaking, one cannot interpret $|\boldsymbol{\Psi}(\mathbf{r},t)|^2$ in terms of photon probability density in position space despite it is a measure of photon energy localization [32–35].

The generalization to N-photon states

$$|\Psi\rangle = \sum_{h_1,\ldots,h_N} \int \mathrm{d}^3k_1 \ldots \int \mathrm{d}^3k_N \; f_{h_1,\ldots,h_N}(\mathbf{k}_1,\ldots,\mathbf{k}_N)|1_{\mathbf{k}_1,h_1},\ldots,1_{\mathbf{k}_N,h_N}\rangle$$

is straightforward. The connection between wave functions and fields is given by

$$\Psi_{i_1\ldots i_N}(q_1,\ldots,q_N) = (-\mathrm{i})^N(2\varepsilon_0)^{N/2}\langle 0|\hat{E}^{(+)}_{i_N}(q_N)\ldots\hat{E}^{(+)}_{i_1}(q_1)|\Psi\rangle \tag{3}$$

and

$$\Psi^*_{i'_1\ldots i'_N}(q'_1,\ldots,q'_N)\Psi_{i_1\ldots i_N}(q_1,\ldots,q_N) = (2\varepsilon_0)^N\,\langle\hat{E}^{(-)}_{i'_1}(q'_1)\ldots\hat{E}^{(-)}_{i'_N}(q'_N)\hat{E}^{(+)}_{i_N}(q_N)\ldots\hat{E}^{(+)}_{i_1}(q_1)\rangle. \tag{4}$$

Eq. (4) shows that *any* field correlation function of a N-photon system can be computed as a product of two tensor elements of the N-photon wave function. As in the one particle case, the N-photon wave-function can be interpreted in terms of photodetection. $\sum_{i_1,\ldots,i_N}|\Psi_{i_1,\ldots,i_N}(q_1,\ldots,q_N)|^2$ is proportional to the joint probability of detecting the photons at space-time points $(q_1,\ldots,q_N)$.

It should be noted that the multi-particle wave functions constructed in this section are different from those that are constructed from the bi-vector form $\overline{\psi}(\mathbf{r},t) = [\boldsymbol{\psi}_+(\mathbf{r},t)\;\boldsymbol{\psi}_-(\mathbf{r},t)]$ of the Bialynicki-Birula-Sipe wave function [36, 37]. The later cannot be directly interpreted in terms of N-photon detection amplitude because they contain a magnetic part to which electric dipole detectors are insensitive. However, since in paraxial approximation the magnetic field carries the same energy as the electric field, the square of both wave functions are proportional. Therefore, joint photo-detection probabilities calculated from vector and bi-vector wave functions are identical.

In [36], it has been shown that the bi-vector form of a Bialynicki-Birula-Sipe wave function satisfies a Maxwell-Dirac differential equation whatever the number of photons N in the system. This equation can be used to study the photon propagation in vacuum, in (not dispersive, possibly inhomogeneous) dielectrics, and at interfaces. It is well suited to study propagation in waveguides or in scattering media such as a turbulent atmosphere as demonstrated in [36]. However, to study the propagation of N photons through a table-top optical setup made of masks, lenses, mirrors and beam-splitter, an integral approach similar to the Huygens-Fresnel principle in coherent optics is more suitable. Such an integral formulation is paraxial and neglects all boundary conditions (in particular reflections at the interfaces of optical elements),

except a set of reference surfaces (usually planes) on which the field values must be specified. We derive such a formulation in the next section.

3. Generalized Huygens-Fresnel principle

We first consider free-space propagation. We make the simplifying assumption that we deal with paraxial states of light, in which case polarization does not change much during propagation. Therefore, we drop the polarization-related indexes. Considering photons propagating along the z-axis, we use the Huygens-Fresnel principle [38] to express $\hat{E}^{(+)}$ at some point as a function of its values on a reference plane Σ_j at z-coordinate ζ_j,

$$\hat{E}^{(+)}(\mathbf{r},t) = \frac{1}{2\pi c}\iint_{\Sigma_j} \mathrm{d}^2\rho_j^{\perp} \frac{\frac{\mathrm{d}}{\mathrm{d}t}\hat{E}^{(+)}(\boldsymbol{\rho}_j, t-\frac{|\mathbf{r}-\boldsymbol{\rho}_j|}{c})}{|\mathbf{r}-\boldsymbol{\rho}_j|}, \tag{5}$$

and inject this in Eq. (3):

$$\Psi(\mathbf{r}_1,t_1,\ldots,\mathbf{r}_N,t_N) = \frac{1}{(2\pi c)^N}\iint_{\Sigma_1}\mathrm{d}^2\rho_1^{\perp}\ldots\iint_{\Sigma_N}\mathrm{d}^2\rho_N^{\perp} \frac{\frac{\mathrm{d}}{\mathrm{d}t_1}\cdots\frac{\mathrm{d}}{\mathrm{d}t_N}\Psi(\boldsymbol{\rho}_1,t_1-\frac{|\mathbf{r}_1-\boldsymbol{\rho}_1|}{c},\ldots,\boldsymbol{\rho}_N,t_N-\frac{|\mathbf{r}_N-\boldsymbol{\rho}_N|}{c})}{|\mathbf{r}_1-\boldsymbol{\rho}_1|\cdots|\mathbf{r}_N-\boldsymbol{\rho}_N|}. \tag{6}$$

Note that, in principle, up to N different reference surfaces can be appear in Eq. (6) – one per occurrence of the $\hat{E}^{(+)}$-field in Eq. (3). For indistinguishable photons, these boundary conditions must be properly symmetrized to leave the wave function unchanged under particle exchange. We call Eq. (6) the generalized Huygens-Fresnel (GHF) principle for N-photon wave functions. In Eqs. (5) and (6), $\boldsymbol{\rho}_j = (\xi_j,\eta_j,\zeta_j)$ ($j\in\{1,\ldots,N\}$) are points in the ζ_j-plane and $\boldsymbol{\rho}_j^{\perp} = (\xi_j,\eta_j)$ are their transverse components. In the optical domain, photons are usually quasi-monochromatic. Therefore, the wave function can be written $\Psi(\mathbf{r}_1,t_1,\ldots,\mathbf{r}_N,t_N) = a(\mathbf{r}_1,t_1,\ldots,\mathbf{r}_N,t_N)\exp(-\mathrm{i}2\pi c(\frac{t_1}{\lambda_1}+\cdots+\frac{t_N}{\lambda_N}))$, where $a(\mathbf{r}_1,t_1,\ldots,\mathbf{r}_N,t_N)$ is a slowly varying function of time and λ_j ($j\in\{1,\ldots,N\}$) are the central wavelengths of the photons. Note that nothing prevents photons from having the same central wavelength or even being indistinguishable. Inserting that anzats in Eq. (6) and taking into account that $a(\mathbf{r}_1,t_1,\ldots,\mathbf{r}_N,t_N)$ is slowly varying in time, one obtains

$$a(\mathbf{r}_1,t_1,\ldots,\mathbf{r}_N,t_N) = \frac{(-\mathrm{i})^N}{\lambda_1\ldots\lambda_N}\iint_{\Sigma_1}\mathrm{d}^2\rho_1^{\perp}\ldots\iint_{\Sigma_N}\mathrm{d}^2\rho_N^{\perp}\frac{\mathrm{e}^{\mathrm{i}\frac{2\pi}{\lambda_1}|\mathbf{r}_1-\boldsymbol{\rho}_1|}}{|\mathbf{r}_1-\boldsymbol{\rho}_1|}\ldots\frac{\mathrm{e}^{\mathrm{i}\frac{2\pi}{\lambda_N}|\mathbf{r}_N-\boldsymbol{\rho}_N|}}{|\mathbf{r}_N-\boldsymbol{\rho}_N|} \times a(\boldsymbol{\rho}_1,t_1-\frac{|\mathbf{r}_1-\boldsymbol{\rho}_1|}{c},\ldots,\boldsymbol{\rho}_N,t_N-\frac{|\mathbf{r}_N-\boldsymbol{\rho}_N|}{c}). \tag{7}$$

If propagation from $\boldsymbol{\rho}_i$ to $\mathbf{r}_i$ is through an optical system, the free space propagator

$$h_{fs}(\mathbf{r}_i,\boldsymbol{\rho}_i) = \frac{-\mathrm{i}}{\lambda_i}\frac{\exp\left(\mathrm{i}\frac{2\pi}{\lambda_i}|\mathbf{r}_i-\boldsymbol{\rho}_i|\right)}{|\mathbf{r}_i-\boldsymbol{\rho}_i|} \tag{8}$$

must be replaced by the appropriate one $h_i(\mathbf{r}_i,\boldsymbol{\rho}_i)$, which can be computed using standard Fourier optics techniques [38]. With this generalization, Eq. (7) becomes

$$a(\mathbf{r}_1,t_1,\ldots,\mathbf{r}_N,t_N) = \iint_{\Sigma_1}\mathrm{d}^2\rho_1^{\perp}\ldots\iint_{\Sigma_N}\mathrm{d}^2\rho_N^{\perp}\,h_1(\mathbf{r}_1,\boldsymbol{\rho}_1)\ldots h_N(\mathbf{r}_N,\boldsymbol{\rho}_N) a(\boldsymbol{\rho}_1,t_1-\frac{l(\mathbf{r}_1,\boldsymbol{\rho}_1)}{c},\ldots,\boldsymbol{\rho}_N,t_N-\frac{l(\mathbf{r}_N,\boldsymbol{\rho}_N)}{c}), \tag{9}$$

where $l(\mathbf{r}_i,\boldsymbol{\rho}_i)$ is the optical path length from $\boldsymbol{\rho}_i$ to $\mathbf{r}_i$. Formula (9) assumes that there is only *one* optical path from $\boldsymbol{\rho}_i$ to $\mathbf{r}_i$. However, interferometers with arms having different path lengths can be placed between $\boldsymbol{\rho}_i$ and $\mathbf{r}_i$. To take this into account, we generalize (9) in the following way:

$$a(\mathbf{r}_1,t_1,\ldots,\mathbf{r}_N,t_N)=\iint_{\Sigma_1}\mathrm{d}^2\rho_1^{\perp}\ldots\iint_{\Sigma_N}\mathrm{d}^2\rho_N^{\perp}$$
$$\sum_{k_1,\ldots,k_N}a(\boldsymbol{\rho}_1,t_1-\frac{l_{k_1}(\mathbf{r}_1,\boldsymbol{\rho}_1)}{c},\ldots,\boldsymbol{\rho}_N,t_N-\frac{l_{k_N}(\mathbf{r}_N,\boldsymbol{\rho}_N)}{c})\;h_1^{(k_1)}(\mathbf{r}_1,\boldsymbol{\rho}_1)\ldots h_N^{(k_N)}(\mathbf{r}_N,\boldsymbol{\rho}_N). \quad (10)$$

The indexes k_i label the different paths from $\boldsymbol{\rho}_i$ to $\mathbf{r}_i$.

That Fourier optics techniques can be applied to multi-photon wave functions has been first noticed in works [26–28]. Compared to these works, the present formulation brings new interesting features: (i) It introduces time in the diffraction integral. This gives a space-time picture of entanglement and enables a time-resolved analysis of N-photon wave packet propagation and detection [39]. Time-resolved detection is already practical with very monochromatic photons emitted by atomic sources [40]. (ii) Eq. (10) shows how to deal with interferometers in quantum imaging set-ups. As seen from Eq. (10), one cannot account for unbalanced interferometers in the propagators only. Placing independent interferometers in the paths of entangled photons makes it possible to explore the spatial and/or multi-particle counterparts of Franson-like interferometry [41]. (iii) The present formalism applies to quantum systems made of an arbitrary number of photons, possibly emitted by sources that are located in *different* transverse planes Σ_j. In schemes that generate N-photon entanglement through multiple nonlinear interactions (up- and down-conversions), the surfaces Σ_j may represent the (thin) nonlinear crystals in which the interaction takes place. The propagation of photons coherently created in these planes, possibly at different times, can be calculated using Eq. (9). An example of such a situation is worked out in Sec. 6.

4. Detection process and wave function reduction

As pointed out in Sec. 2, $|\Psi(q_1,\ldots,q_N)|^2$ is proportional to the joint detection probability to detect the N photons at points $q_1=(\mathrm{r}_1,t_1)$ to $q_N=(\mathrm{r}_N,t_N)$. What happens when a photon is indeed detected at point q_N^*? In contrast to standard detection theory, the quantum state of the N^{th} is not projected on a localized state $|q_N^*\rangle$ but rather on vacuum $|0\rangle$ since the photon disappears. Therefore photodetection process should be modeled by the projection operator $|0\rangle\langle q_N^*|$ acting on the N photon quantum state $|\Psi\rangle$. In terms of position wave functions, this simply means that the N-particle wave function $\Psi(q_1,\ldots,q_N)$ is instantaneously reduced to a $(N-1)$-particle wave function $\Psi(q_1,\ldots,q_{N-1}|q_N^*)$ in which q_N^* is not a variable anymore. It is important to realize that the quantum state is still a *pure* state after the detection of one of its photons. Therefore, starting with $N+M$ photons, it is possible to *shape* a desired N-photon wave function by designing an appropriate detection scheme for the M ancillary photons. An example illustrating this point will be developed in Sec. 5.

The situation is different if "bucket" detectors are used. Such detector record the arrival time but not the position of the detected photon. If the N^{th} photon of a N-photon system is detected in a bucket detector at time t_N^*, the remaining $N-1$ photons are projected on a mixed quantum state. The joint detection probability of the remaining photons at points $q_1=(\mathrm{r}_1,t_1)$ to $q_{N-1}=(\mathrm{r}_{N-1},t_{N-1})$ is given by $\int_{\mathscr{D}}|\Psi(q_1,\ldots,q_{N-1}|r_N^*,t_N^*)|^2\mathrm{d}r_N^*$, where $\mathscr{D}$ is the region in which the N^{th} photon could have been detected. As pointed out before for biphotons [27], this probability usually differs from the one obtained by simply tracing over the degrees of freedom of the N^{th} photon.

5. Shaping the wave function through the detection process: application to super-resolution imaging

To illustrate how the reduction of a three photon state can be used to shape the wave function of the remaining two photons, consider the set-up of Fig. 1. A multi-step nonlinear process as in [20] produces photon triplets in a thin nonlinear crystal. We assume perfect energy and momentum conservation, so that the photon triplets are entangled in space and time. In the plane of the device:

$$a(\boldsymbol{\rho}_1,t_1,\boldsymbol{\rho}_2,t_2,\boldsymbol{\rho}_3,t_3) = E(t_3)\,F(\boldsymbol{\rho}_3^{\perp})\,\delta(\boldsymbol{\rho}_1^{\perp}-\boldsymbol{\rho}_3^{\perp})\,\delta(\boldsymbol{\rho}_2^{\perp}-\boldsymbol{\rho}_3^{\perp})\,\delta(t_1-t_3)\,\delta(t_2-t_3),$$

where E and F define the temporal and transverse width of the 3-photon wave function. A dichroic beam splitter (DBS) separates two degenerate photons (wavelength λ_1) from the third one (wavelength λ_2). In the λ_1 output, two thin lenses (focal f_1 and f_3) image the output of the crystal to the object plane O first (magnification $M = s_2/(s_0+s_1)$), then to the D_a-detector plane (D_a is a two-photon detector). The single-photon detector D_b is placed on the optical axis. Using formula (9), one can calculate the 3-photon amplitude in the O- and D_b-planes. If a photon is detected by D_b at time t_*, the wave function of the λ_1 photons is projected on (see Sec. 4)

$$\begin{aligned} a(\mathbf{r},t,\mathbf{r}',t') =& \delta(t-(t_*+\tau))\,\delta(t-t')\,\delta(\mathbf{r}^{\perp}-\mathbf{r}'^{\perp})F(\mathbf{r}^{\perp}/M) \\ & \exp\left(\mathrm{i}2\pi|\mathbf{r}^{\perp}|^2(1+1/M)/(\lambda_1 s_2)\right)\,h_2(0,-\mathbf{r}/M). \end{aligned}$$

where $\tau = (s_1+s_2-s_3-s_4)/c$ and $h_2(\mathbf{r}_b,\boldsymbol{\rho}_3)$ is the propagator from the nonlinear device to the detector D_b. This state is a linear superposition of localized two-photon Fock states of light. It has been shown [42] that illuminating an object with such a state enables coherent super-resolution imaging of the object with a diffraction-limited lens f_3 and a point-like detector D_a. To get a good quality image, controlling the phase-curvature of the illuminating beam is also crucial [43]. The scheme makes it possible to control the wavefront curvature of the λ_1 2-photon state by tailoring the detection of the λ_2 photon. For instance, one can make the wave front of λ_1 photons flat in the object plane by placing a lens (focal f_2) in the path to D_2 (see Fig. 1) and choosing s_3, s_4 and f_2 so that $2(\lambda_2/\lambda_1)M(M+1) = s_2/((1/f_2-1/s_4)^{-1}-(s_0+s_3))$. This solution exists if the inequalities $s_4(s_0+s_3)/(s_0+s_3+s_4) < f_2 < s_4$ are satisfied. In this way, a phase accumulated by the λ_1 photons is cancelled by a phase accumulated by the λ_2 photon.

By moving the detector D_b along the z-axis, other wave-front curvatures can be produced. In addition, by moving this detector transversally one creates a tilt in the direction of propagation of the λ_1 photons. If the plane O and the detector D_b are in distant laboratories (O in Bob's laboratory and D_b in Alice's laboratory), Alice can remotely generate a given 2-photon state at

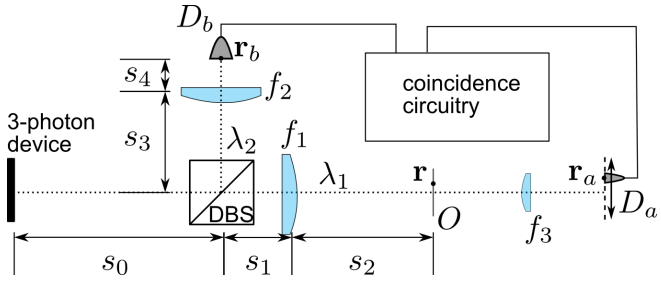

Fig. 1. Generation of heralded linear superposition of localized two-photon states of light.

Bob's side, conditionally to the detection of the λ_2 photons at the appropriate position. Such a procedure is an example of a *remote state preparation* protocol (RSP). RSP is similar to quantum teleportation (QT) in the sense that in both cases Alice wants to send a quantum state to Bob. The difference with QT is that in RSP Alice knows the state that she want to transmit to Bob. Recently, an efficient method for remotely preparing spatial qubits has been designed [44, 45]. In another publication, a teleportation of the entire angular spectrum of a single photon has been reported [46]. In the setup of Fig. 1, the spatial profile of the bi-photon at λ_1 will be quasi-Gaussian. Therefore, the tilt controls the propagation axis of the beam and the wavefront curvature controls its beam waist. The waist position is the only parameter that Alice cannot control independently. If she communicates to Bob one real number – the offset Bob needs to apply to his reference frame in order to have the beam waist at the right z-coordinate – she could create at Bob's site any Gaussian beam. This RSP requires an entangled state and the communication of a real number. This simple protocol can probably be improved to reduce the amount of the required classical communication.

6. Entangled images

To illustrate how to apply the GHF principle when the photons are generated in two different nonlinear crystals, consider the scheme of Fig. 2. A pump pulse is split in two parts using a 50/50 beam splitter (BS). The two pump parts are coherent and produce non degenerated collinear photon pairs (at λ_1 and λ_2) in two different non linear crystals (NLC) Γ_1 and Γ_2. Two dichroic mirrors are used to separate λ_1 and λ_2 photons. Finally, photons at λ_1 are made to interfere on a second 50/50 BS and are detected using two point-like single-photon detectors, D_a and D_b, placed on the optical axis. Note that we call z the coordinate along the optical axis independently of its direction changes due to the BSs and DBSs.

Assuming that the crystals are thin and that the pump pulse is a quasi-plane wave, the 4-

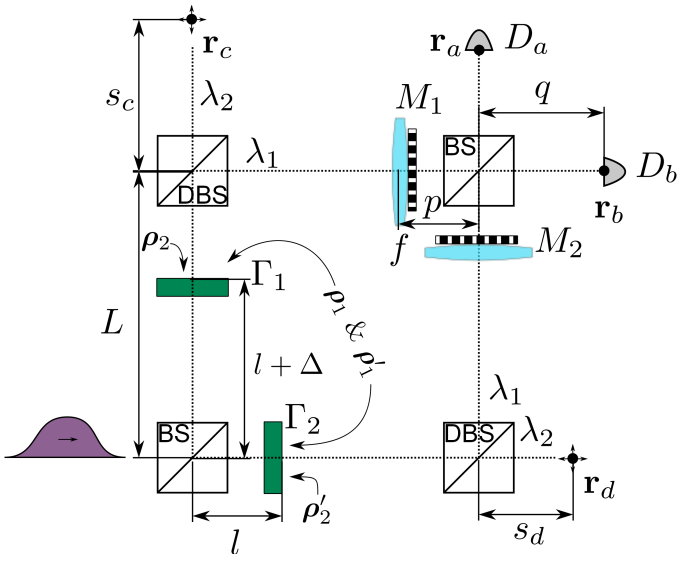

Fig. 2. Scheme for quantum imaging with two independent photon pairs.

photon position wave function generated in the NLCs reads

$$a(\boldsymbol{\rho}_1,t_1,\boldsymbol{\rho}_2,t_2,\boldsymbol{\rho}'_1,t'_1,\boldsymbol{\rho}'_2,t'_2) = E(t_2)E(t'_2+\Delta/c)\Big(\delta(t_1-t_2)\delta(t'_1-t'_2)\delta(\boldsymbol{\rho}_1^{\perp}-\boldsymbol{\rho}_2^{\perp})\delta(\boldsymbol{\rho}'^{\perp}_1-\boldsymbol{\rho}'^{\perp}_2) + \delta(t'_1-t_2)\delta(t_1-t'_2)\delta(\boldsymbol{\rho}'^{\perp}_1-\boldsymbol{\rho}_2^{\perp})\delta(\boldsymbol{\rho}_1^{\perp}-\boldsymbol{\rho}'^{\perp}_2)\Big) \tag{11}$$

where $E(t)$ is the temporal profile function of the pump wave. Eq. (11) assumes a perfect momentum conservation between the pump, the signal and the idler photons during the nonlinear generation process: $|\Psi\rangle = \sum_{i,s}\delta(\omega_s+\omega_i-\omega_p)\delta(\mathbf{k}_s+\mathbf{k}_i-\mathbf{k}_p)|\mathbf{k}_s\rangle|\mathbf{k}_i\rangle$ (see [18]). Changing from the momentum to the position basis, it turns out that the signal and idler photons must originate from the same scattering point in the crystal. Another way of arriving to that conclusion in explained in [47], where the theory of spontaneous parametric down-conversion is explained in the wave function formalism. The wave function has been symmetrized with respect to the coordinates $\boldsymbol{\rho}_1$ and $\boldsymbol{\rho}'_1$ of the λ_1 photons. This symmetrization is necessary because, if a λ_1 photon is detected at $\mathbf{r}_a$ (or $\mathbf{r}_b$) there no way to know if it came from one NLC or the other one (see Fig. 2). No symmetrization with respect to the λ_2 photons is needed because their is no ambiguity about their origin when they are detected at $\mathbf{r}_c$ and $\mathbf{r}_d$. We assumed that the NLCs are placed at different positions (Δ) in the two arms of the setup in Fig. 2 to stress that geometrical symmetry is not required to made the λ_1 photon indistinguishable.

The propagation to the points $\mathbf{r}_a$, $\mathbf{r}_b$, $\mathbf{r}_c$, and $\mathbf{r}_d$ can be computed using the GHF intergral (9):

$$\begin{aligned} a(\mathbf{r}_a,t_a,\mathbf{r}_b,t_b,\mathbf{r}_c,t_c,\mathbf{r}_d,t_d) = &\iint_{\Gamma_1\cup\Gamma_2}\mathrm{d}^2\rho_1^{\perp}\iint_{\Gamma_1}\mathrm{d}^2\rho_2^{\perp}\iint_{\Gamma_1\cup\Gamma_2}\mathrm{d}\rho'^{\perp}_1\iint_{\Gamma_2}\mathrm{d}\rho'^{\perp}_2 \\ &h_a(\mathbf{r}_a,\boldsymbol{\rho}_1)\,h_b(\mathbf{r}_b,\boldsymbol{\rho}'_1)\,h_c(\mathbf{r}_c,\boldsymbol{\rho}_2)\,h_d(\mathbf{r}_d,\boldsymbol{\rho}'_2) \\ a(\boldsymbol{\rho}_1,t_a-\frac{l(\mathbf{r}_a,\boldsymbol{\rho}_1)}{c},&\boldsymbol{\rho}_2,t_c-\frac{l(\mathbf{r}_c,\boldsymbol{\rho}_2)}{c},\boldsymbol{\rho}'_1,t_b-\frac{l(\mathbf{r}_b,\boldsymbol{\rho}'_1)}{c},\boldsymbol{\rho}'_2,t_d-\frac{l(\mathbf{r}_d,\boldsymbol{\rho}'_2)}{c}). \end{aligned} \tag{12}$$

Note that according to Fig. 2, the integration surfaces for coordinates $\boldsymbol{\rho}_2$ and $\boldsymbol{\rho}'_2$ are the non linear crystal planes Γ_1 and Γ_2. However for coordinates $\boldsymbol{\rho}_1$ and $\boldsymbol{\rho}'_1$ the integration surface is $\Gamma_1\cup\Gamma_2$ since those coordinates represent photons that cannot be distinguished by the detection scheme. Inserting the two photon amplitude (11) into Eq. (12), one gets:

$$\begin{aligned} a(\mathbf{r}_a,t_a,\mathbf{r}_b,t_b,\mathbf{r}_c,t_c,\mathbf{r}_d,t_d) = &E(t_c-\tau_1)\,E(t_d-\tau_1)\Big[\delta(t_a-t_c-\tau_2)\,\delta(t_b-t_d-\tau'_2) \\ &\iint_{\Gamma_1}d^2\rho\iint_{\Gamma_2}d^2\rho' h_a(\mathbf{r}_a,\boldsymbol{\rho})\,h_b(\mathbf{r}_b,\boldsymbol{\rho}')\,h_c(\mathbf{r}_c,\boldsymbol{\rho})\,h_d(\mathbf{r}_d,\boldsymbol{\rho}')\Big] \\ &+\delta(t_b-t_c-\tau_2)\,\delta(t_a-t_d-\tau_2) \\ &\iint_{\Gamma_1}d^2\rho\iint_{\Gamma_2}d^2\rho' h_a(\mathbf{r}_a,\boldsymbol{\rho}')\,h_b(\mathbf{r}_b,\boldsymbol{\rho})\,h_c(\mathbf{r}_c,\boldsymbol{\rho})\,h_d(\mathbf{r}_d,\boldsymbol{\rho}')\Big], \end{aligned} \tag{13}$$

where $\tau_1 = (L+s_c-(l+\Delta))/c$ is the propagation delay from the NLC Γ_1 to the detector $\mathbf{r}_c$, while $\tau_2 = (L+q-s_c)/c$ and $\tau'_2 = (L+q-s_d)/c$ are the propagation delay difference between the λ_1 and the λ_2 photons to their respective detectors. As expected, the detections of the λ_2 photons are usually not synchronous although they happen during a time bin equal to the pump duration. However, a detection of the λ_2 photons at times t_c and t_d heralds the arrival of the λ_1 photons at times $t_c+\tau_2$ and $t_d+\tau'_2$. Unless the λ_2 photons are detected at times t_c and t_d such that $t_d = t_c+\tau_2-\tau'_2$, the λ_1 photons are distinguishable by their arrival time (measuring the

arrival time of the photon detected at $\mathbf{r}_a$ reveals NLC it originates from). By post-selecting only coincidence detection events at space-time point $(\mathbf{r}_c, t_*)$ and $(\mathbf{r}_d, t_* + \tau_2 - \tau_2')$ the two-photon wave function of the λ_1 photons is projected on

$$a(\mathbf{r}_a, t_a, \mathbf{r}_b, t_b) = E^2(t_* - \tau_1)\delta(t_a - t_* - \tau_2)\delta(t_a - t_b)\left[\phi_{ac}(\mathbf{r}_a)\ \phi_{bd}(\mathbf{r}_b) + \phi_{ad}(\mathbf{r}_a)\ \phi_{bc}(\mathbf{r}_b)\right], \quad (14)$$

where

$$\phi_{ac}(\mathbf{r}_a) = \iint_{\Gamma_1} h_a(\mathbf{r}_a, \boldsymbol{\rho})\ h_c(\mathbf{r}_c, \boldsymbol{\rho}) d^2\rho, \quad (15a)$$

$$\phi_{ad}(\mathbf{r}_a) = \iint_{\Gamma_2} h_a(\mathbf{r}_a, \boldsymbol{\rho}')\ h_d(\mathbf{r}_d, \boldsymbol{\rho}') d^2\rho', \quad (15b)$$

$$\phi_{bd}(\mathbf{r}_b) = \iint_{\Gamma_2} h_b(\mathbf{r}_b, \boldsymbol{\rho}')\ h_d(\mathbf{r}_d, \boldsymbol{\rho}') d^2\rho', \quad (15c)$$

$$\phi_{bc}(\mathbf{r}_b) = \iint_{\Gamma_1} h_b(\mathbf{r}_b, \boldsymbol{\rho})\ h_c(\mathbf{r}_c, \boldsymbol{\rho}) d^2\rho. \quad (15d)$$

Such a state is a pure entangled two-particle state, although not a maximally entangled Bell-state since photon position wave functions are not restricted to a two-dimensional Hilbert space. Furthermore, by designing the propagators h_α ($\alpha \in \{a, b, c, d\}$), a large variety of entangle states can be produced. In particular, if the propagation from the last BS to the detectors $\mathbf{r}_a$ and $\mathbf{r}_b$ is identical, $h_a(\mathbf{r}_a, \boldsymbol{\rho}) = \mathrm{i}\ h_b(\mathbf{r}_b, \boldsymbol{\rho})$ and $h_a(\mathbf{r}_a, \boldsymbol{\rho}') = -\mathrm{i}\ h_b(\mathbf{r}_b, \boldsymbol{\rho}')$. As a result, $\phi_{ac}(\mathbf{r}) = \mathrm{i}\ \phi_{bc}(\mathbf{r}) \equiv \phi_1(\mathbf{r})$, $\phi_{bd}(\mathbf{r}) = -\mathrm{i}\ \phi_{ad}(\mathbf{r}) \equiv \phi_2(\mathbf{r})$, and the quantum state (14) becomes similar to the $|\Psi^+\rangle$ Bell-state:

$$a(\mathbf{r}_a, t_a, \mathbf{r}_b, t_b) = E^2(t_* - \tau_1)\delta(t_a - t_* - \tau_2)\delta(t_a - t_b)\left[\phi_1(\mathbf{r}_a)\ \phi_2(\mathbf{r}_b) + \phi_2(\mathbf{r}_a)\ \phi_1(\mathbf{r}_b)\right]. \quad (16)$$

As seen from Eq. (16), the scheme of Fig. 2 realises an entanglement swapping in the spatial domain. An heralded entangled photon pairs is produced from a 4-particle state of light. However in contrast with standard qubit entanglement swapping [48], entanglement is produced between *continuous-variable* states that live in infinite-dimensional Hilbert space. Such states have applications in continuous variable quantum information processing. As shown earlier, protocols initially designed for multi-photon field quadrature variables (for instance [49]) can be efficiently implemented using (x, k) variables of single-photon fields [50–52]. Entangled qudits can also be produced by restricting the photon state to a d-dimensional linear subspace of the full Hilbert space, as has been recently investigated by many authors [9, 53, 54].

The specific arrangement of Fig 2 is made of two positive lenses (focal length f) and two complex transmission masks (M_1 and M_2). The arrangement is such that the detectors $\mathbf{r}_a$ and $\mathbf{r}_b$ are in the Fourier planes of the lenses *relatively to the two-photon imaging* conditions. In other words, we assume that the following two-photon lens law is satisfied:

$$\frac{1}{\mathscr{L}} + \frac{1}{p+q} = \frac{1}{f}, \quad (17)$$

with

$$\mathscr{L} = (2L - l - \Delta - p) + \frac{\lambda_2}{\lambda_1}(L - l - \Delta + s_c)) = (2L - l - p) + \frac{\lambda_2}{\lambda_1}(L - l + s_d)). \quad (18)$$

Note that the second equality in Eq. (18) can only be satisfied simultaneously with the first one if

$$s_c - s_d = \frac{\lambda_1 + \lambda_2}{\lambda_2}\Delta. \quad (19)$$

The length $\mathscr{L}$ is the propagation length from $\mathbf{r}_c$ to the crystal Γ_1 (and from $\mathbf{r}_d$ to the crystal Γ_2), then from the crystal to the lens in the geometrical optics interpretation of two photon-imaging [18]. We also assume that the detection points $\mathbf{r}_c$ and $\mathbf{r}_d$ lay on the optical axis.

The two-photon detection amplitude at detectors $\mathbf{r}_a$ and $\mathbf{r}_b$ can be deduced from Eqs. (15) and (16), after calculating the propagators h_α ($\alpha \in \{a,b,c,d\}$) using standard Fourier optics techniques [38]. The result of the calculation is

$$\begin{aligned}\phi_1(\mathbf{r}) =& \frac{-1}{\lambda_1^2 \mathscr{L}(p+q)} \exp\left[\mathrm{i}\frac{2\pi}{\lambda_1}(2L-l-\Delta+q)\right] \exp\left[\mathrm{i}\frac{2\pi}{\lambda_2}(L-l-\Delta+s_c)\right] \\ & \exp\left[\mathrm{i}\frac{\pi}{\lambda_1}\frac{x^2+y^2}{p+q}\right] \tilde{M}_1\left(\frac{x}{\lambda_1(p+q)}, \frac{y}{\lambda_1(p+q)}\right)\end{aligned} \tag{20}$$

and

$$\begin{aligned}\phi_2(\mathbf{r}) =& \frac{-1}{\lambda_1^2 \mathscr{L}(p+q)} \exp\left[\mathrm{i}\frac{2\pi}{\lambda_1}(2L-l+q)\right] \exp\left[\mathrm{i}\frac{2\pi}{\lambda_2}(L-l+s_d)\right] \\ & \exp\left[\mathrm{i}\frac{\pi}{\lambda_1}\frac{x^2+y^2}{p+q}\right] \tilde{M}_2\left(\frac{x}{\lambda_1(p+q)}, \frac{y}{\lambda_1(p+q)}\right),\end{aligned} \tag{21}$$

where

$$\tilde{M}_\alpha(\xi,\eta) = \iint \mathrm{d}x\mathrm{d}y\, M_\alpha(x,y)\, \exp\left[-\mathrm{i}2\pi(x\xi+y\eta)\right] \tag{22}$$

is the spatial Fourier transform of the mask M_α ($\alpha \in \{1,2\}$). Therefore

$$a(\mathbf{r}_a,t_a,\mathbf{r}_b,t_b) = E^2(t_*-\tau_1)\delta(t_a-t_*-\tau_2)\delta(t_a-t_b)\left[\tilde{M}_1(\mathbf{r}_a)\,\tilde{M}_2(\mathbf{r}_b)+\tilde{M}_2(\mathbf{r}_a)\,\tilde{M}_1(\mathbf{r}_b)\right] \tag{23}$$

up to constant or irrelevant phase factors. By designing the complex masks M_1 and M_2, one can prepare any two-photon position-entangled state of light. Moreover, since this scheme relies on entanglement swapping, the photon pair is heralded. We call the state (23) an entangled-image state because each photon that is detected is in a quantum superposition of two different images, but joint detections are correlated.

7. Conclusion

In summary, we explored the physics of quantum imaging with $N > 2$. By quantum imaging, we mean processing the photons through arbitrary optical systems (made of lenses, beams splitters, apertures, complex modulation masks) that modify the wave fronts of the single-photon wave functions and possibly projects the N-photon state on a M-photon state ($M < N$)) by detecting some of the particles. We present a general and self-consistent formalism that describes the (paraxial) propagation of multi-photon states in position representation and uses methods closely related the Huygens-Fresnel principle and Fourier techniques in coherent optics. Compared to the bi-photon physics (entangled photons produced by parametric down-conversion), some delicate issues appear in the general N-photon case when photons are generated coherently in different places (two separate non-linear crystal, for instance) but nevertheless become indistinguishable by propagating in the optical system. We show how to deal with such problems when computing the propagation of the N-photon quantum state and illustrate this situation by describing a scheme that performs a continuous-variable entanglement-swapping between two photon pairs generated in two different nonlinear crystals. The resulting heralded two-photon state displays entanglement in the position space: each photon is in a superposition of two different field distributions, with perfect anti-correlation: $\phi_1(\mathbf{r}_a)\,\phi_2(\mathbf{r}_b)+\phi_2(\mathbf{r}_a)\,\phi_1(\mathbf{r}_b)$. We expect both the general formalism and the worked out examples to stimulate new design of N-photon sources with engineered spatial entanglement.

Acknowledgements

This research was supported by the Interuniversity Attraction Poles program, Belgium Science Policy, under grant P6-10 and the Fonds de la Recherche Scientifique - FNRS (F.R.S.-FNRS, Belgium) under the FRFC grant 2.4.638.09F.